



**Optimizing the linear electron transport rate measured by chlorophyll a fluorescence to empirically match the gross rate of oxygen evolution in white light: Towards improved estimation of the cyclic electron flux around Photosystem I in leaves**

Journal:	<i>Functional Plant Biology</i>
Manuscript ID	FP18039.R1
Manuscript Type:	Research paper
Date Submitted by the Author:	n/a
Complete List of Authors:	Zhang, Meng-Meng; Northeast Forestry University, Harbin, College of Life Science Fan, Da-Yong; Australian National University, Research School of Biology Sun, Guang-Yu; Northeast Forestry University, Harbin, College of Life Science Chow, Wah Soon; Australian National University, Research School of Biology
Keyword:	Chlorophyll fluorescence, Electron transport, Photosystem I, Photosystem II, Bioenergetics, Light reactions

SCHOLARONE™  
Manuscripts

1

2 **Optimizing the linear electron transport rate measured by chlorophyll *a***  
3 **fluorescence to empirically match the gross rate of oxygen evolution in white**  
4 **light: Towards improved estimation of the cyclic electron flux around**  
5 **Photosystem I in leaves**

6

7 Meng-Meng Zhang<sup>A,B</sup>, Da-Yong Fan<sup>B</sup>, Guang-Yu Sun<sup>A,C</sup> and Wah Soon Chow<sup>B,C</sup>

8 <sup>A</sup>College of Life Science, Northeast Forestry University, Harbin, Heilongjiang,  
9 150040, China.

10 <sup>B</sup>Division of Plant Sciences, Research School of Biology, The Australian National  
11 University, Acton, ACT 2601, Australia.

12 <sup>C</sup>Corresponding author. E-mail: [Fred.Chow@anu.edu.au](mailto:Fred.Chow@anu.edu.au); [sungy@vip.sina.com](mailto:sungy@vip.sina.com)

13

14

15 **Running title:** Optimizing matching of fluorescence- and O<sub>2</sub>-based electron transport  
16 rates

17

18 **Abbreviations:** AA, antimycin A; CEF, cyclic electron flux around PS I; Chl,  
19 chlorophyll;  $\Delta\text{Flux}$ , difference between ETR1 and ETR2 as an estimate of CEF;  
20 ETR1, the electron flux through PS I; ETR2, the electron flux through PS II (and PS I  
21 in series) measured as either  $\text{LEF}_n$  or  $\text{LEF}_{\text{O}_2}$ ;  $f_I$ , and  $f_{\text{II}}$ , the fraction of absorbed light  
22 partitioned to PS I and PS II, respectively;  $F_m$  and  $F_m'$ , the maximum Chl fluorescence  
23 yield in a dark-adapted state and a light-adapted state, respectively;  $F_s$  and  $F_o'$ , the  
24 steady-state and minimum Chl fluorescence yield in a light-adapted state, respectively;  
25  $I$ , irradiance;  $\text{LEF}_n$ , the linear electron flux through both photosystems, measured by  
26 chlorophyll fluorescence;  $\text{LEF}_{\text{O}_2}$ , the linear electron flux through both photosystems,  
27 measured by the gross rate of oxygen evolution; MV, methyl viologen; NDH,  
28 nicotinamide adenine dinucleotide dehydrogenase-like complex; P700, the special Chl  
29 pair acting as the primary electron donor in PSI; PGR5, proton gradient regulation 5  
30 protein;  $P_m$  and  $P_m'$ , signal corresponding to the maximum extent of oxidizable P700  
31 in weak far-red light and in actinic light, respectively; PS I and PS II, Photosystem I  
32 and II, respectively;  $qP$ , the photochemical quenching parameter;  $Y(\text{I})$  and  $Y(\text{II})$ , the  
33 photochemical yield of PS I and PS II, respectively.

#### 34 **Summary Text for the Table of Contents**

35 Cyclic electron flow around Photosystem I (CEF) was discovered in isolated  
36 chloroplasts more than six decades ago, but its quantification has been elusive. We  
37 devised a method capable of estimating CEF in intact leaves attached to a plant. The  
38 method involves measurement of (1) the total electron flux through Photosystem I by

39 a near-infra-red signal, and (2) the linear electron flux through both photosystems in  
40 series by optimizing conditions of excitation and detection of chlorophyll  
41 fluorescence.

## 42 **Abstract**

43 The cyclic electron flux (CEF) around photosystem I (PSI) was discovered in isolated  
44 chloroplasts more than six decades ago, but its quantification has been hampered by  
45 the absence of net formation of a product or net consumption of a substrate. We  
46 estimated *in vivo* CEF in leaves as the difference ( $\Delta\text{Flux}$ ) between the total electron  
47 flux through PSI (ETR1) measured by a near infra-red signal, and the linear electron  
48 flux through both photosystems by optimized measurement of chlorophyll *a*  
49 fluorescence ( $\text{LEF}_{\text{fl}}$ ). Chlorophyll fluorescence was excited by modulated green  
50 light from a light-emitting diode at an optimal average irradiance, and the  
51 fluorescence was detected at wavelengths  $>710$  nm. In this way,  $\text{LEF}_{\text{fl}}$  matched the  
52 gross rate of oxygen evolution multiplied by 4 ( $\text{LEF}_{\text{O}_2}$ ) in broad-spectrum white  
53 actinic irradiance up to half (spinach, poplar and rice) or one-third (cotton) of full  
54 sunlight irradiance. This technique of estimating CEF can be applied to leaves  
55 attached a plant.

## 56 **Introduction**

57 Although discovered six decades ago (Arnon *et al.* 1955, Shikanai 2007), the cyclic  
58 electron flux around Photosystem I (PSI) is difficult to quantify because there is  
59 neither net formation of a product nor net consumption of a substrate. Currently, a

60 reasonable estimation involves measuring the total electron flux through PSI (ETR1)  
61 and the linear electron flux through both photosystems in series under identical  
62 illumination and sampling conditions. That is, ETR1 is measured by the redox  
63 signal of P700, the primary electron donor in PSI in the form of a chlorophyll (Chl)  
64 dimer in leaves. To obtain ETR1, the photochemical yield of PSI,  $Y(I)$ , given by the  
65 fraction of P700 that can potentially be photo-oxidized under a given set of  
66 measurement conditions (Klughammer and Schreiber 1994, 2007), was first  
67 determined;  $Y(I)$  can then be used to calculate ETR1 by taking into account the  
68 irradiance, leaf absorbance and the fraction of absorbed light partitioned to PSI ( $f_I$ ),  
69 as well as assuming the quantum efficiency of photochemical conversion to be 1.0.  
70 The linear electron flux through PSII and PSI in series (ETR2) was measured by the  
71 gross rate of oxygen evolution using a Clarke-type oxygen electrode in CO<sub>2</sub>-enriched  
72 air in which photorespiration is suppressed (LEF<sub>O<sub>2</sub></sub>). Both ETR1 and LEF<sub>O<sub>2</sub></sub> are  
73 measurements representative of the whole leaf tissue: oxygen is evolved from PSII  
74 complexes that absorb light anywhere within the tissue, while the measuring beam for  
75 detecting the P700<sup>+</sup> signal (820 nm, with reference wavelength 870 nm), being only  
76 weakly absorbed by P700<sup>+</sup> and hardly absorbed by neutral chlorophyll (Chl)  
77 molecules, is scattered repeatedly in the whole tissue until it is absorbed by P700<sup>+</sup>  
78 (Oguchi *et al.* 2011).

79 The difference  $ETR1 - LEF_{O_2} = \Delta Flux$  is approximately the cyclic electron  
80 flux (CEF) if photorespiration and the local electron cycle in PSI in the form of  
81 charge recombination are negligible. Alternatively, if oxygen evolution is assayed

82 by membrane-inlet mass spectrometry, the oxygen uptake in photorespiratory  
83 conditions can be taken into account; the method can then be used in ambient air  
84 (although the draw-down of CO<sub>2</sub> in a closed chamber rapidly changes the [CO<sub>2</sub>] in  
85 ambient air), provided charge recombination in PSI is negligible. However,  
86 membrane-inlet mass spectrometry is not as readily available as a Clarke-type oxygen  
87 electrode.

88 Another disadvantage associated with oxygen measurement is that a leaf  
89 segment is cut and placed in a chamber, either that of an oxygen electrode or that of a  
90 mass spectrometer, making *in situ* measurement of leaves attached to a plant  
91 impossible. A further disadvantage is that, since oxygen measurements are generally  
92 slow, there is limited time resolution to monitor the time course of CEF, for example,  
93 during photosynthetic induction. Thus, assaying linear electron flux by oxygen  
94 measurement can present a number of shortcomings (Fan *et al.* 2016).

95 The linear electron flux (ETR<sub>2</sub>) through both photosystems can also be measured  
96 by Chl *a* fluorescenc, which yields the photochemical yield of PSII, Y(II). Y(II) can  
97 then be used to calculate ETR<sub>2</sub> (specifically termed LEF<sub>II</sub> here) by taking into account  
98 the irradiance, leaf absorptance and  $f_{II}$  the fraction of absorbed light partitioned to  
99 PSII (Genty *et al.* 1989; Evans *et al.* 2017). Chl fluorescence can be measured on a  
100 leaf attached to a plant, in photorespiratory conditions and with good time resolution.  
101 Unfortunately, without optimizing the conditions of Chl fluorescence measurement,  
102 ETR<sub>2</sub> so obtained can be considerably less than LEF<sub>O<sub>2</sub></sub> in broad-spectrum white

103 actinic light, when the modulated measuring (excitation) light is blue (Kou *et al.*  
104 2013). This underestimation of the linear electron flux is due to the inherently  
105 localized detection of the Chl fluorescence signal from a shallow depth of the leaf  
106 tissue (Oguchi *et al.* 2011). Under other conditions, where the *actinic* light is blue  
107 but the modulated measuring light is red, Chl fluorescence-based ETR2 can be  
108 considerably *greater* than the linear electron transport rate obtained from the gross  
109 rate of CO<sub>2</sub> assimilation (Evans *et al.* 2017); this observation can be explained by a  
110 multilayer photosynthesis model (Evans 2009; Evans *et al.* 2017). The aim of this  
111 present study is to select conditions in which LEF<sub>fl</sub> is more representative of the  
112 whole tissue, so that it can match LEF<sub>O<sub>2</sub></sub>, both measured in broad-spectrum white light;  
113 LEF<sub>fl</sub> can then be subtracted from ETR1 to yield a reasonable estimate of CEF. This  
114 method allows us to estimate CEF in leaves attached to a plant even in  
115 photorespiratory conditions, at least up to a certain actinic irradiance, as demonstrated  
116 in four plant species.

## 117 **Materials and methods**

### 118 **Plant growth**

119 Four plant species, *Spinacia oleracea* L. (cv. Yates hybrid 102), *Populus canadensis*  
120 cv. 'Evergreen 65-1', *Oryza sativa* L. (spp. Japonica) and *Gossypium hirsutum* L. (cv.  
121 Sicot 75), were grown in a glasshouse (~30/15 °C, day/night); they represent,  
122 *respectively*, various plant types: herbaceous, woody, monocot, and *a perennial plant*  
123 *that is usually grown as an annual crop*. A nutrient mix (Aquasol, Hortico, Clayton,

124 Australia) was supplemented by a slow release fertilizer ('Osmocote', Scotts Australia  
125 Pty Ltd, Castle Hill). Young fully-expanded leaves were used for measurements.

#### 126 **Measurements of O<sub>2</sub> evolution**

127 O<sub>2</sub> evolution from leaf discs was measured in a gas-phase oxygen electrode  
128 (Hansatech, King's Lynn, UK) chamber maintained at 25°C. The sample chamber  
129 contained 1% CO<sub>2</sub> supplied by fabric matting moistened with 1 M NaHCO<sub>3</sub>/Na<sub>2</sub>CO<sub>3</sub>  
130 (pH = 9). O<sub>2</sub> evolution was measured in continuous white light from a halogen lamp  
131 (400-740 nm, peak spectral irradiance 620 nm, with about 7% of the irradiance within  
132 the wavelength range 700-740 nm) over several minutes until steady state. The  
133 slope at approximately 40 s after cessation of illumination (when a cooling artefact  
134 had subsided) was subtracted algebraically from the steady-state net oxygen evolution  
135 rate to yield the *gross* oxygen evolution rate. The gross oxygen evolution rate was  
136 multiplied by 4 to obtain the linear electron flux LEF<sub>O<sub>2</sub></sub>. The actinic irradiance was  
137 varied by increasing it in steps from darkness to yield a light-response curve. For  
138 calibration of the oxygen signals, 1 mL of air at 25°C (taken to contain 8.05 μmol O<sub>2</sub>)  
139 was injected into the gas-phase O<sub>2</sub> electrode chamber.

#### 140 **Measurement of Chl *a* fluorescence**

141 A pulse amplitude modulation fluorometer PAM 101/103 (Walz, Effeltrich, Germany)  
142 was used to measure Y(II). The modulated excitation light (1.6 kHz, unless  
143 automatically switched to 100 kHz when the saturating pulse was applied) was either



144 blue (wavelength 462 nm, average irradiance =  $0.05 \mu\text{mol m}^{-2} \text{s}^{-1}$ ), red (wavelength  
145 665 nm,  $0.05 \mu\text{mol m}^{-2} \text{s}^{-1}$ ) or green (wavelength 511 nm, up to  $0.38 \mu\text{mol m}^{-2} \text{s}^{-1}$ ).  
146 To obtain sufficient green excitation irradiance, several commercial green LEDs were  
147 tested. The chosen green LED (Cree C503B-GAN 535 nm Green LED) was the  
148 brightest, and was driven by an amplified (modulated) voltage from the Emitter  
149 terminal of the PAM 101. A stainless-steel metal mesh, of the kind used in a  
150 Hansatech oxygen electrode, was placed underneath a leaf disc or a leaf attached to a  
151 plant, to reflect green excitation light back into the leaf tissue, while allowing gas  
152 diffusion in and out of the abaxial side.

153 A saturating pulse of white light, of duration 0.8 s and irradiance  $7,300 \mu\text{mol m}^{-2}$   
154  $\text{s}^{-1}$ , was used to obtain the maximum Chl fluorescence yield in a dark-adapted sample  
155 ( $F_m$ ) or a light-adapted sample ( $F_m'$ ). In retrospective tests of saturation by the pulse  
156 of white light, we compared  $\text{LEF}_{\text{fl}}$  obtained using a saturating pulse of irradiance  
157  $12,000 \mu\text{mol m}^{-2} \text{s}^{-1}$  or  $7,300 \mu\text{mol m}^{-2} \text{s}^{-1}$ . The increases in  $\text{LEF}_{\text{fl}}$  (using an average  
158 green excitation irradiance of  $0.24 \mu\text{mol m}^{-2} \text{s}^{-1}$ ) that we obtained at  $12,000 \mu\text{mol m}^{-2}$   
159  $\text{s}^{-1}$  compared with  $7,300 \mu\text{mol m}^{-2} \text{s}^{-1}$  were at most (at the actinic irradiance  $1,500 \mu\text{mol}$   
160  $\text{m}^{-2} \text{s}^{-1}$ ) only slight for spinach (2%), poplar (4%), rice (4%) and cotton (5%). Below  
161  $1,000 \mu\text{mol m}^{-2} \text{s}^{-1}$ , (spinach, poplar and rice) or  $600 \mu\text{mol m}^{-2} \text{s}^{-1}$  (cotton), there was  
162 no statistical difference between  $12,000 \mu\text{mol m}^{-2} \text{s}^{-1}$   $7,300 \mu\text{mol m}^{-2} \text{s}^{-1}$ . Thus, we  
163 consider a pulse at  $7,300 \mu\text{mol m}^{-2} \text{s}^{-1}$  to be saturating for the actinic irradiance range  
164 relevant to this study.

165 The Chl fluorescence was measured via the Detector terminal of the PAM 101  
166 (Walz, Effeltrich, Germany), using a filter which transmitted fluorescence of  
167 wavelength >710 nm. The rationale of selecting longer wavelengths is the  
168 expectation that re-absorption of long-wavelength fluorescence would be minimized,  
169 thereby allowing detection from greater depths in the tissue.

170 The photochemical yield of PSII,  $Y(II)$ , was calculated as  $1 - F_s/F_m'$ , where  $F_s$  is  
171 the steady-state fluorescence yield and  $F_m'$  the maximum fluorescence yield in the  
172 light-adapted state (Genty *et al.* 1989). The fluorescence-based linear rate of  
173 electron transport through PSII (and PSI) was calculated as  $LEF_{II} = Y(II) \times I \times 0.85 \times$   
174  $0.5$ , where  $I$  is the irradiance, 0.85 the leaf absorptance and 0.5 the assumed  
175 partitioning (also see experimental estimations in Table 1) of the absorbed light  
176 between the two photosystems.

177 The photochemical quenching parameter  $qP$  was calculated as  $(F_m' - F_s)/(F_m' -$   
178  $F_o')$ , where  $F_o'$  is the minimum Chl fluorescence yield of open PSII reaction centre  
179 traps in the light-adapted state.  $F_o'$  was calculated according to Oxborough and  
180 Baker (1997).

### 181 **Measurement of the P700<sup>+</sup> signal from leaf segments**

182 Measurement of the photochemical yield of PSI,  $Y(I)$ , is based on the technique of  
183 Klughammer and Schreiber (1994, 2007), slightly modified by introducing a strong  
184 far-red pulse shortly before the saturating pulse of white light, as described by Kou *et*  
185 *al.* (2013). The measurement employed a dual-wavelength (820/870 nm) P700 unit

186 (ED-P700DW) connected to a pulse amplitude modulation (PAM 101) fluorometer  
187 (Walz, Effeltrich, Germany) in the reflectance mode, with a metal mesh underneath  
188 the abaxial side of a leaf segment inside a gas-phase oxygen electrode in which the  
189 upper water jacket had a vertical port for accepting a multifurcated light guide.  
190 When a leaf attached to the plant was sampled, the same upper water jacket was  
191 placed on the leaf, with the metal mesh underneath the leaf. The metal mesh served  
192 to reflect the near-infra-red measuring beam or the fluorescence excitation light back  
193 to the leaf tissue, while allowing gas diffusion into the abaxial side of the leaf.  
194 Actinic illumination was provided to the adaxial side of the leaf disc. Timing of data  
195 acquisition and application of various lights was controlled by a pulse-delay generator  
196 (Model 555, Berkeley Nucleonics, San Rafael, CA, USA).

197 The measurement of  $Y(I)$  was conducted in two stages (Kou *et al.* 2013). First,  
198 a leaf sample was illuminated to steady state for about 10 minutes during which  
199 oxygen evolution or Chl fluorescence was monitored. Then the system was quickly  
200 (within  $< 1$  min during which the leaf sample was in darkness) switched to P700<sup>+</sup>  
201 measurement. To re-establish steady state, the leaf sample was illuminated with a  
202 given actinic light for 8.8 s before data acquisition started, followed by a strong  
203 far-red pulse ( $600 \mu\text{mol m}^{-2} \text{s}^{-1}$ , 100 ms duration), in the middle of which a saturating  
204 pulse ( $10,000 \mu\text{mol m}^{-2} \text{s}^{-1}$ , 10 ms duration) was applied to reach the maximum  
205 permissible oxidation of P700 ( $P_m'$ ) in the presence of actinic light. The duration of  
206 total actinic illumination was 9.0 s. The sequence was repeated every 9.3 s, so that  
207 the dark time (which helped to establish the baseline corresponding to fully reduced

208 P700) between repeats was about 3.2% of the total length of time. Twenty-five  
209 repeat signals were averaged.

210 The second stage of Y(I) measurement was to determine the maximum signal  
211 corresponding the maximum P700 photo-oxidation when the acceptor-side limitation  
212 was negligible. Weak far-red light ( $92 \mu\text{mol m}^{-2} \text{s}^{-1}$ ) was applied to attain a steady  
213 P700<sup>+</sup> concentration. Then a saturating pulse (0.5 ms duration,  $10,000 \mu\text{mol m}^{-2} \text{s}^{-1}$ )  
214 was applied to fully oxidize the remaining P700 ( $P_m$ ). The values of  $P_m$ ,  $P_m'$ , and the  
215 steady-state oxidation state of P700 in the presence of a given actinic light were used  
216 to calculate Y(I) according to Klughammer and Schreiber (2007).

## 217 **Results**

### 218 **Light-response curves of photosynthetic electron transport determined via gross** 219 **oxygen evolution and via the yield of Chl *a* fluorescence excited by blue, red or** 220 **green modulated light**

221 The gross rate of oxygen evolution, in white halogen light and in 1% CO<sub>2</sub>, of spinach  
222 leaf discs cut from plants grown in a glasshouse showed typical responses. At the  
223 maximum irradiance of almost  $1,700 \mu\text{mol m}^{-2} \text{s}^{-1}$  tested, the gross rate of oxygen  
224 evolution multiplied by 4 (LEF<sub>O2</sub>) was nearly, but not yet fully, light-saturated (Fig. 1,  
225 closed circles). LEF<sub>O2</sub> was compared with the fluorescence-based LEF<sub>fl</sub>. Fig. 1  
226 shows that the extent of matching of LEF<sub>fl</sub> with LEF<sub>O2</sub> varied with irradiance and with  
227 wavelength of the modulated excitation light. At low actinic irradiance, below about

228  $500 \mu\text{mol m}^{-2} \text{s}^{-1}$ , the matching was good regardless of excitation wavelength.  
229 Above this irradiance, however, the matching was the poorest with blue, and then red  
230 excitation light. Matching was improved with green excitation light; at an average  
231 excitation irradiance of  $0.38 \mu\text{mol m}^{-2} \text{s}^{-1}$ , the matching was better than with  $0.05$   
232  $\mu\text{mol m}^{-2} \text{s}^{-1}$ . However, above actinic irradiance  $1,100 \mu\text{mol m}^{-2} \text{s}^{-1}$ , the  
233 fluorescence-based  $\text{LEF}_{\text{fl}}$  underestimated the linear electron flux obtained as  $\text{LEF}_{\text{O}_2}$ .

234 Similarly, poplar leaf discs in 1%  $\text{CO}_2$  showed poor matching of  $\text{LEF}_{\text{O}_2}$  and  $\text{LEF}_{\text{fl}}$   
235 obtained in blue excitation light, slightly better matching in red excitation light, and  
236 somewhat better matching with weak green excitation light ( $0.07 \mu\text{mol m}^{-2} \text{s}^{-1}$ , Fig.  
237 2a). In another batch of poplar plants, matching was good at an average green  
238 excitation irradiance of  $0.38 \mu\text{mol m}^{-2} \text{s}^{-1}$ , up to an actinic irradiance of  $\sim 1,000 \mu\text{mol}$   
239  $\text{m}^{-2} \text{s}^{-1}$  (Fig. 2b). At even higher green excitation irradiance, the matching  
240 deteriorated (data not shown).

241 In rice leaf segments measured in 1%  $\text{CO}_2$ , the matching was similarly improved  
242 as the green excitation light increased to  $0.38 \mu\text{mol m}^{-2} \text{s}^{-1}$  (Fig. 3). However, when  
243 the actinic irradiance exceeded  $\sim 1,100 \mu\text{mol m}^{-2} \text{s}^{-1}$ , the matching deteriorated,  $\text{LEF}_{\text{fl}}$   
244 being considerably smaller than  $\text{LEF}_{\text{O}_2}$ .

245 In cotton leaf discs measured in 1%  $\text{CO}_2$ , the matching also improved as the  
246 excitation light was changed from blue to red to green. However, the matching was  
247 not good when the actinic irradiance exceeded  $\sim 700 \mu\text{mol m}^{-2} \text{s}^{-1}$ , even with green  
248 excitation light. This maximum actinic irradiance for good matching is lower in

249 cotton than in the other three plant species.

250 **Estimation of cyclic electron flux around PSI as the difference ( $\Delta\text{Flux}$ ) between**  
251 **ETR1 and  $\text{LEF}_{\text{fl}}$**

252 Given the reasonably good matching between  $\text{LEF}_{\text{fl}}$  and  $\text{LEF}_{\text{O}_2}$  when Chl *a*  
253 fluorescence was excited by green light at  $0.38 \mu\text{mol m}^{-2} \text{s}^{-1}$  and in white actinic light  
254 of irradiance  $< 1,000 \mu\text{mol m}^{-2} \text{s}^{-1}$  (spinach, poplar and rice leaves), or  $< 700 \mu\text{mol}$   
255  $\text{m}^{-2} \text{s}^{-1}$  (cotton leaves), we proceeded to estimate cyclic electron flux around PSI as  
256 the difference ( $\Delta\text{Flux}$ ) between ETR1 and  $\text{LEF}_{\text{fl}}$ . These electron fluxes were  
257 determined on intact leaves attached to the plant in air, or in leaf discs in air enriched  
258 with 1%  $\text{CO}_2$ , the latter conditions used in oxygen measurements. In spinach leaves  
259 attached to the plant in air,  $\text{LEF}_{\text{fl}}$  was not yet saturated at  $1,100 \mu\text{mol m}^{-2} \text{s}^{-1}$ , and  
260 ETR1 was even less light-saturated (Fig. 5a).  $\Delta\text{Flux}$ , was very small (relative to  
261  $\text{LEF}_{\text{fl}}$ ) at irradiance  $< 300 \mu\text{mol m}^{-2} \text{s}^{-1}$ ; above  $500 \mu\text{mol m}^{-2} \text{s}^{-1}$ , however, it increased  
262 steadily until, at  $1,000 \mu\text{mol m}^{-2} \text{s}^{-1}$ , it was about one-third of  $\text{LEF}_{\text{fl}}$ . Similar results  
263 for  $\Delta\text{Flux}$  were obtained with spinach leaf discs in 1%  $\text{CO}_2$  (Fig. 5b).

264 Spinach leaf discs were vacuum infiltrated with water (control),  $200 \mu\text{M}$   
265 antimycin A (AA, an inhibitor of the PGR5-dependent cyclic pathway) or  $100 \mu\text{M}$   
266 methyl viologen (MV, a mediator of electron transfer to molecular oxygen). Excess  
267 intercellular water was allowed to evaporate in darkness until the tissue was no longer  
268 translucent, before measurements. Table 2 shows that  $\Delta\text{Flux}$  was close to zero after  
269 these treatments.

270 In an intact poplar leaf attached to a cut branch of a plant,  $\Delta\text{Flux}$  was very small  
271 (relative to  $\text{LEF}_{\text{fl}}$ ) in white actinic light below actinic irradiance  $100 \mu\text{mol m}^{-2} \text{s}^{-1}$ ,  
272 above which it increased practically linearly (Fig. 6a). In cut leaf discs in 1%  $\text{CO}_2$ ,  
273  $\Delta\text{Flux}$  increased in the same way as in the intact leaf, even though  $\text{ETR1}$  was  
274 somewhat smaller at high actinic irradiance, and  $\text{LEF}_{\text{fl}}$  showed a slight decline at high  
275 actinic irradiance (Fig. 6b).

276 In rice leaves attached to the plant,  $\Delta\text{Flux}$  was negligibly small (relative to  $\text{LEF}_{\text{fl}}$ )  
277 below actinic irradiance  $200 \mu\text{mol m}^{-2} \text{s}^{-1}$ . It then increased linearly up to the  
278 maximum actinic irradiance  $1,100 \mu\text{mol m}^{-2} \text{s}^{-1}$ , at which it reached 62% of  $\text{LEF}_{\text{fl}}$   
279 (Fig. 7a). In **cut** rice leaf segments in 1%  $\text{CO}_2$  (Fig. 7b), both  $\text{ETR1}$  and  $\text{LEF}_{\text{fl}}$  were  
280 smaller than in intact leaves. Nonetheless,  $\Delta\text{Flux}$  behaved similarly as in intact  
281 leaves.

282 In cotton leaves, we had to restrict the actinic irradiance to below  $800 \mu\text{mol m}^{-2}$   
283  $\text{s}^{-1}$  for matching of  $\text{LEF}_{\text{O}_2}$  and  $\text{LEF}_{\text{fl}}$ . The  $\text{LEF}_{\text{fl}}$  so obtained was similar in an intact  
284 leaf attached to the plant in air **to that of** a leaf disc in 1%  $\text{CO}_2$  (Fig. 8). In either  
285 case,  $\Delta\text{Flux}$  (relative to  $\text{LEF}_{\text{fl}}$ ) was negligibly small below  $100 \mu\text{mol m}^{-2} \text{s}^{-1}$ , but **it**  
286 increased linearly above that irradiance.  $\Delta\text{Flux}$  was slightly larger in an intact cotton  
287 leaf than in a cut leaf disc.

#### 288 **The decrease in $\text{LEF}_{\text{fl}}$ at high actinic irradiance**

289 At high actinic irradiance,  $\text{LEF}_{\text{fl}}$  decreased in all four species, resulting in a deviation

290 from the  $LEF_{O_2}$  curve. To investigate the reason behind the decrease in  $LEF_{fl}$ , we  
291 plotted  $qP \times I$  (the product of the photochemical quenching parameter and irradiance)  
292 against irradiance (Fig. 9a) in cotton leaves. It is seen that  $qP \times I$  increased rapidly  
293 with irradiance, then more slowly and even decreased slightly at irradiance  $>700$   
294  $\mu\text{mol m}^{-2} \text{s}^{-1}$ , implying that  $qP$  decreased more drastically than irradiance increased.  
295 By contrast, a plot of  $(F_v'/F_m') \times I$  (the product of the light-adapted ratio of variable  
296 fluorescence to maximum fluorescence and irradiance) against irradiance is a nearly  
297 straight line, implying that  $F_v'/F_m'$  was relatively constant.

## 298 DISCUSSION

299 One method of estimation of CEF involves determination of both the electron flux  
300 through PSI (ETR1) and the linear electron flux ( $LEF_{O_2}$ ) through both photosystems  
301 in series under identical conditions (Kou *et al.* 2013). Determination of  $LEF_{O_2}$  in an  
302 oxygen electrode necessitates the use of a high  $\text{CO}_2$  concentration to suppress  
303 photorespiration and the cutting of a leaf segment or disc to be placed in the electrode  
304 chamber. Further, oxygen measurements are inherently slow and, therefore, unable  
305 to follow changes in CEF with sufficient time resolution, for example, during  
306 photosynthetic induction. These shortcomings prompted us to seek an alternative  
307 method of determining the linear electron flux.

308 Chlorophyll *a* fluorescence potentially offers such a convenient and  
309 non-intrusive technique: it can be applied to an intact leaf attached to a plant, in air,  
310 and with good resolution time. Various studies have attempted to correlate Chl *a*



311 fluorescence parameters with gas-exchange measurements. For instance, Weis and  
312 Berry (1987) obtained a linear plot of  $\phi_{O_2}/qP$  against  $qN$ , where  $\phi_{O_2}$  is the gross rate of  
313 oxygen evolution divided by the irradiance  $I$ ,  $qP$  is a photochemical quenching  
314 parameter and  $qN$  is a non-photochemical quenching parameter. In principle,  
315 measurements of  $qP$ ,  $qN$  and  $I$  should yield the gross rate of oxygen evolution from an  
316 equation fitted to the linear plot. Unfortunately, the relationship is not universal  
317 among leaves of plants; there are occasional exceptions to a single straight line  
318 (Öquist and Chow 1992).

319 Genty *et al.* (1987) reported a near-linear relation between  $Y(II)$  and  $\phi_{CO_2}$ , the  
320  $CO_2$  assimilation rate per unit irradiance in barley and maize, as did Edwards and  
321 Baker (1993) in maize. Seaton and Walker (1990) and Öquist and Chow (1992), on  
322 the other hand, observed a curvilinear relation between  $Y(II)$  and  $\phi_{O_2}$ , the gross  $O_2$   
323 evolution rate per unit irradiance. Further, there were exceptions to what appeared at  
324 first sight to be a universal relation that can be fitted by a single curve (Öquist and  
325 Chow 1992). The difficulty of obtaining a universal relation between Chl  
326 fluorescence measurements and gas-exchange measurements is no doubt due to the  
327 differential sampling of the leaf tissue by the two techniques: oxygen is evolved from  
328 the whole tissue, but the fluorescence is predominantly detected from chloroplasts  
329 near the surface of the leaf facing the detector. For this reason, fluorescence-derived  
330  $LEF_{fl}$  depends on the spectral quality of the measuring beam, that of the actinic light,  
331 and the wavelength band over which the fluorescence is detected (Evans *et al.* 2017).  
332 By attempting to optimize the fluorescence measurement in this study, we hoped to

333 obtain a signal that is more representative of the whole leaf tissue and, therefore,  
334 better matched with gas exchange measurements, at least up to a certain actinic  
335 irradiance.

### 336 **Optimizing $LEF_{fl}$ to match $LEF_{O_2}$**

337 We used green excitation light which is attenuated more slowly as it penetrates the  
338 leaf tissue (Terashima *et al.* 2009) and which, therefore, reports from greater depths in  
339 the leaf tissue. We also detected Chl fluorescence at wavelengths  $\geq 710$  nm; the  
340 long-wavelength emission, if occurring from deep tissue, is less likely to be  
341 re-absorbed by chlorophyll on its way to the detector. Using these measurement  
342 conditions, we obtained  $LEF_{fl} = Y(II) \times I \times 0.85 \times 0.5$ , as explained in Methods. The  
343 assumed partitioning of the absorbed, broad-spectrum halogen light between the two  
344 photosystems is 0.5 to each photosystem. For spinach grown in a glasshouse, this  
345 was indeed the case experimentally (Fan *et al.* 2016). Below, we experimentally  
346 obtain the partitioning of broad-spectrum halogen light for the four species, all grown  
347 in the same glasshouse. It is noted that at low actinic irradiance ( $\leq 500$  for spinach  
348 and rice;  $\leq 150 \mu\text{mol m}^{-2} \text{s}^{-1}$  for cotton and poplar), the variation of  $LEF_{fl}$  with actinic  
349 irradiance was practically independent of the spectral quality and/or irradiance of the  
350 weak excitation light. This is probably because, at a relatively low actinic irradiance,  
351 only the chloroplasts in shallow leaf tissue were photosynthesizing to any great extent.  
352 Under such conditions, by simply equating  $Y(II) \times I \times 0.85 \times f_{II}$  with  $LEF_{O_2}$  for  
353 irradiance  $\leq 150 \mu\text{mol m}^{-2} \text{s}^{-1}$  (poplar and cotton) or  $\leq 500 \mu\text{mol m}^{-2} \text{s}^{-1}$  (spinach and

354 rice), we derived values of  $f_{II}$  as shown in Table 1. The average  $f_{II}$  is very close to  
355 0.5, justifying our use of the value of  $f_{II} = 0.5$  for the partitioning to PSII and  $f_I = 0.5$   
356 for the partitioning to PSI in the four species, in broad-spectrum white light.

357 The linear electron flux detected by Chl fluorescence  $LEF_{F_0}$  flows through both  
358 photosystems in series, to reduce  $NADP^+$  to NADPH or, to a much lesser extent in  
359 angiosperms, reduce  $O_2$  to form superoxide in the Mehler reaction. The linear  
360 electron flux detected as oxygen evolution  $LEF_{O_2}$ , on the other hand, would be  
361 underestimated if oxygen were simply consumed in the Mehler reaction. However,  
362 the resulting superoxide is scavenged in the water-water cycle to release oxygen again  
363 (Asada 2000, Miyake 2010); therefore, no net consumption of oxygen occurs despite  
364 any Mehler reaction, and  $LEF_{O_2}$  correctly measures the linear electron flux through  
365 both photosystems even when the Mehler reaction occurs, provided the water-water  
366 cycle runs efficiently. Thus, neither  $LEF_{F_0}$  nor  $LEF_{O_2}$  is compromised by any Mehler  
367 reaction.

368 At high actinic irradiance it is obvious that, to obtain good matching between  
369  $LEF_{F_0}$  and  $LEF_{O_2}$ , excitation with blue light was not as good as with red light, which  
370 was not as good as with green light; further, a higher average excitation irradiance of  
371 green light, up to about  $0.38 \mu\text{mol m}^{-2} \text{s}^{-1}$ , seemed to be optimal. (Figs. 1-4). Thus,  
372 using this green optimal irradiance for the measuring beam, there was good matching  
373 of  $LEF_{O_2}$  and  $LEF_{F_0}$  up to a broad-spectrum actinic irradiance of  $\sim 1,000 \mu\text{mol m}^{-2} \text{s}^{-1}$   
374 for spinach, rice and poplar, and about  $700 \mu\text{mol m}^{-2} \text{s}^{-1}$  for cotton leaves.

375 Beyond the maximum actinic irradiance below which the matching was good,  
376  $LEF_{fl}$  decreased slightly, even when  $LEF_{O_2}$  continued to increase with irradiance.  
377 This discrepancy between  $LEF_{fl}$  and  $LEF_{O_2}$  at high actinic irradiance prompted us to  
378 re-measure  $LEF_{fl}$  using two saturating pulses, one at irradiance  $12,000 \mu\text{mol m}^{-2} \text{s}^{-1}$ ,  
379 and the other at  $7,300 \mu\text{mol m}^{-2} \text{s}^{-1}$  which was originally used. The increases in  $LEF_{fl}$   
380 (using an average green excitation irradiance of  $0.24 \mu\text{mol m}^{-2} \text{s}^{-1}$ ) that we obtained at  
381  $12,000 \mu\text{mol m}^{-2} \text{s}^{-1}$  compared with  $7,300 \mu\text{mol m}^{-2} \text{s}^{-1}$  were at most (at the actinic  
382 irradiance  $1,500 \mu\text{mol m}^{-2} \text{s}^{-1}$ ) only slight for spinach (2%), poplar (4%), rice (4%) and  
383 cotton (5%) (Data not shown). These differences, while real, are not sufficient to  
384 explain the discrepancy between  $LEF_{fl}$  and 4 x the gross oxygen evolution rate at  
385 actinic irradiance  $1,500 \mu\text{mol m}^{-2} \text{s}^{-1}$  (13% for spinach, 28% for poplar, 17% for rice  
386 and 28% for cotton). In all four plant species, no significant difference in  $LEF_{fl}$   
387 between the two saturating pulse intensities was obtained when the actinic irradiance  
388 was below a certain value:  $1,000 \mu\text{mol m}^{-2} \text{s}^{-1}$  for spinach, rice and poplar, and  $660$   
389  $\mu\text{mol m}^{-2} \text{s}^{-1}$  for cotton. That is, a pulse at  $7,300 \mu\text{mol m}^{-2} \text{s}^{-1}$  was saturating at or  
390 below these irradiances; these are also actinic irradiance values below which we  
391 obtained a good empirical matching of  $LEF_{fl}$  and  $LEF_{O_2}$ .

392 The slight decrease in  $LEF_{fl}$  at high actinic irradiance is almost certainly due to  
393 detection of the fluorescence predominantly from chloroplasts in shallower depths of  
394 the tissue. In shallow tissue the actinic irradiance is not yet attenuated substantially,  
395 and  $Q_A$  is in a more reduced state ( $qP$  lower) than is the case in deeper tissue.  
396 Indeed, plotting the product of  $qP$  and  $I$  against  $I$  gave a curve that reached a

397 maximum at an irradiance at which  $LEF_{\text{fl}}$  began to deviate from  $LEF_{\text{O}_2}$  (Fig. 9a).  
398 Above that maximum irradiance,  $qP \times I$  even declined slightly with increase in  
399 irradiance. Since  $LEF_{\text{fl}} = Y(\text{II}) \times I \times 0.85 \times f_{\text{fl}}$ , where  $Y(\text{II}) = qP \times F_v'/F_m'$ , there is  
400 an underestimation of  $LEF_{\text{fl}}$  due to the use of a  $qP$  that represents chloroplasts in  
401 shallower depths of the tissue rather than in the whole tissue. By contrast to  $qP$ , the  
402 photochemical yield of open PSII reaction centre traps ( $F_v'/F_m'$ ) was rather constant,  
403 since a plot of the product of  $F_v'/F_m'$  and  $I$  against  $I$  yielded a near-straight line (Fig.  
404 9b).

#### 405 **Estimation of CEF from the difference between ETR1 and $LEF_{\text{fl}}$**

406 Since Chl fluorescence can be measured from a leaf attached to a plant, and since  
407  $LEF_{\text{fl}}$  and  $LEF_{\text{O}_2}$  can be empirically matched, at least up to a certain maximum actinic  
408 irradiance, we are in a position to estimate CEF as the difference between ETR1 and  
409  $LEF_{\text{fl}}$  in intact spinach leaves in air. Fig. 5a shows ETR1 increasing with irradiance,  
410 even when  $LEF_{\text{fl}}$  began to plateau. The difference ( $\Delta\text{Flux}$ ) is attributable mainly to  
411 CEF, since  $\Delta\text{Flux}$  at  $980 \mu\text{mol m}^{-2} \text{s}^{-1}$  in spinach leaf discs is almost completely  
412 inhibited by antimycin A (Kou *et al.* 2013) and completely abolished by antimycin A  
413 or MV as shown in Table 2. At  $980 \mu\text{mol m}^{-2} \text{s}^{-1}$ ,  $\Delta\text{Flux}$  (= ETR1 -  $LEF_{\text{fl}}$ ) was  
414 approximately one-third of  $LEF_{\text{fl}}$  in an intact spinach leaf (Fig. 5a), just as  $\Delta\text{Flux}$  (in  
415 that case the difference between ETR1 and  $LEF_{\text{O}_2}$ ) was about one-third of  $LEF_{\text{O}_2}$  in  
416 leaf discs in 1%  $\text{CO}_2$  (Kou *et al.* 2013). Further, at actinic irradiance  $<300 \mu\text{mol m}^{-2}$   
417  $\text{s}^{-1}$ ,  $\Delta\text{Flux}$  was very small relative to  $LEF_{\text{fl}}$ , just there was little  $\Delta\text{Flux}$  at low actinic

418 irradiance when compared with  $LEF_{O_2}$  (Kou et al. 2013). There was little difference  
419 between the  $\Delta Flux$  of an intact spinach leaf in air in the laboratory environment and  
420 that of leaf discs in 1%  $CO_2$ .

421  $\Delta Flux$  in spinach leaf discs after vacuum infiltration with antimycin A (AA) was  
422 close to zero at both 500 and 1,000  $\mu mol m^{-2} s^{-1}$  (Table 2). This suggests that AA  
423 inhibited the PGR5-dependent CEF pathway completely. Further, this result  
424 indicates that, in spinach, there was little or no charge recombination in PSI at these  
425 irradiances, for any charge recombination would have contributed to a residual  $\Delta Flux$ .  
426 In *Arabidopsis thaliana*, the NDH-dependent pathway is minor compared with the  
427 PGR5-dependent CEF pathway and NDH may even aid the AA-sensitive,  
428 PGR5-dependent CEF pathway (Kou et al. 2015). In the presence of MV,  $\Delta Flux$  was  
429 also close to zero. MV, by mediating electron transfer to molecular oxygen, should  
430 have minimized both CEF and charge recombination, so this result was expected.  
431 Unfortunately, we were not able to use vacuum infiltration on leaf tissues of the other  
432 three species without losing photosynthetic activity. Uptake through the cut petioles  
433 of poplar and cotton leaves overnight was attempted, as was floating leaf discs on  
434 solutions, but we were not confident that the inhibitors were reaching all the intended  
435 sites of action.

436 In intact poplar leaves attached to a branch (Fig. 6a) and in cotton leaves  
437 attached to the plant (Fig. 8a),  $\Delta Flux$  increased with actinic irradiance with a smaller  
438 lag ( $< 100 \mu mol m^{-2} s^{-1}$ ) than in the other two species. The same was true of leaf

439 discs in 1% CO<sub>2</sub> (Fig. 6b). The decrease in LEF<sub>fl</sub> at high actinic irradiance was more  
440 pronounced in leaf discs than in an intact leaf. This could be due to some water loss  
441 which resulted in tissue contraction of leaf discs, thereby exacerbating the difficulty  
442 of detecting the fluorescence from the chloroplasts in deeper tissue.

443 ETR1 was greater in intact rice leaves compared with leaf segments, as was  
444 the case of LEF<sub>fl</sub>. This observation confirms that measurements on intact leaves are  
445 superior to those on leaf discs of some plant species, and justifies the search for a  
446 method, such as Chl fluorescence in this study, that allows measurements on an intact  
447 system. Possibly, linear electron transport in rice segments was decreased by  
448 stomatal closure associated with water loss from the cut tissue (Fig. 7). In intact rice  
449 leaves in air as well as leaf segments in 1% CO<sub>2</sub>, a lag (up to ~200 μmol m<sup>-2</sup> s<sup>-1</sup>) was  
450 also apparent before ΔFlux increased steadily with irradiance (Fig. 7). At 1,000  
451 μmol m<sup>-2</sup> s<sup>-1</sup>, ΔFlux was comparable to LEF<sub>fl</sub> in cut leaf segments, whereas it was  
452 only about 60% of LEF<sub>fl</sub> in intact leaves. This could be due to water loss from leaf  
453 segments; water deficit increases CEF as estimated in various ways (Golding *et al.*  
454 2004; Kohzuma *et al.* 2009; Kou *et al.* 2013), despite a decrease in linear electron  
455 transport.

456 Cotton leaf discs showed matching of LEF<sub>O2</sub> and LEF<sub>fl</sub> up to a lower maximum  
457 actinic irradiance than the other three species, so we measured ETR1 and LEF<sub>fl</sub> only  
458 up to 800 μmol m<sup>-2</sup> s<sup>-1</sup>. Above ~100 μmol m<sup>-2</sup> s<sup>-1</sup>, ΔFlux increased steadily in both  
459 intact cotton leaves attached to the plant and in leaf discs in 1% CO<sub>2</sub>, reaching ≥ 50%

460 of  $LEF_{fl}$  at the highest irradiance,  $800 \mu\text{mol m}^{-2} \text{s}^{-1}$ . Cyclic electron transport is a  
461 significant contributor to (1) the resistance of cotton to high-light stress, facilitating  
462 movement of cotton leaves to track the sun and intercept more radiation (Yao *et al.*  
463 2018) and (2) improving the stability of the two photosystems under mild water  
464 deficit conditions (Yi *et al.* 2018).

465 In summary, we selected conditions of measurement so that  $LEF_{fl}$  matched  $LEF_{O_2}$   
466 quite closely, but only up a certain maximum irradiance of actinic light supplied from  
467 a halogen lamp. Up to this maximum actinic irradiance, it is possible to estimate  
468 CEF as the difference ( $\Delta\text{Flux}$ ) between ETR1 and  $LEF_{fl}$  in leaves attached the plant.

#### 469 **Acknowledgements**

470 The authors declare no conflicts of interest. This work was supported by a China  
471 Scholarship Council Fellowship (to M-M Z), and a grant from the Australian  
472 Research Council (to WSC, DP1093827). We thank Adam Pynt for modifying the  
473 PAM 101 to enable excitation with green light. We are grateful to Reviewer 4 for  
474 pointing out the need to test the effect of a much more intense saturating pulse.

475



476 **References**

477 Arnon DI, Whatley FR, Allen MB (1955) Vitamin K as a cofactor of photosynthetic  
478 phosphorylation. *Biochimica et Biophysica Acta* **16**, 607-608

479 Asada K (2000) The water–water cycle as alternative photon and electron sinks.  
480 *Philosophical Transactions of the Royal Society of London B: Biological Sciences*  
481 **355**, 1419–1431

482 Edwards GE, Baker NR (1993) Can CO<sub>2</sub> assimilation in maize leaves be predicted  
483 accurately from chlorophyll fluorescence analysis? *Photosynthesis Research* **37**,  
484 89-102

485 Evans JR (2009) Potential errors in electron transport rates calculated from  
486 chlorophyll fluorescence as revealed by a multilayer model. *Plant & Cell*  
487 *Physiology* **50**, 698-706

---

488 Evans JR, Morgan PB, von Caemmerer S (2017) Light quality affects chloroplast  
489 electron transport rates estimated from Chl fluorescence measurements. *Plant &*  
490 *Cell Physiology* **58**, 1652-1660

491 Fan, DY, Fitzpatrick D, Oguchi R, Ma W, Kou J and Chow WS (2016) Obstacles in  
492 the quantification of the cyclic electron flux around Photosystem I in leaves of C3  
493 plants. *Photosynthesis Research* **129**, 239-251

494 Genty B, Briantais J-M, Baker NR (1989) The relationship between the quantum yield  
495 of photosynthetic electron transport and quenching of chlorophyll fluorescence.  
496 *Biochimica et Biophysica Acta* **990**, 87-92

497 Golding AJ, Finazzi G, Johnson GN (2004) Reduction of the thylakoid electron  
498 transport chain by stromal reductants – evidence for activation of cyclic electron

- 499 transport upon dark adaptation or under drought. *Planta* **220**, 356-363
- 500 Klughammer C, Schreiber U (1994) An improved method, using saturating light  
501 pulses, for the determination of photosystem I quantum yield via P700<sup>+</sup>-absorbance  
502 changes at 830 nm. *Planta* **192**, 261-268
- 503 Klughammer C, Schreiber U (2007) Saturation Pulse method for assessment of energy  
504 conversion in PS I. [http://www.walz.com/e\\_journal/pdfs/PAN07002.pdf](http://www.walz.com/e_journal/pdfs/PAN07002.pdf)
- 505 Kohzuma K, Cruz JA, Akashi K, Hoshiyasu S, Munekage YN, Yokota A, Kramer DM  
506 (2009) The long-term responses of the photosynthetic proton circuit to drought.  
507 *Plant Cell and Environment* **32**, 209-219
- 508 Kou J, Takahashi S, Oguchi R, Fan D-Y, Badger MR, Chow WS (2013) Estimation of  
509 the steady-state cyclic electron flux in white light, CO<sub>2</sub>-enriched air and other  
510 varied conditions. *Functional Plant Biology* **40**, 1018-1028
- 511 Kou J, Takahashi S, Fan D-Y, Badger MR, Chow WS (2015) Partially dissecting the  
512 steady-state electron fluxes in Photosystem I in wild-type and *pgr5* and *ndh*  
513 mutants of *Arabidopsis*. *Frontiers in Plant Science* **6**, Article 758
- 
- 514 Miyake C (2010) Alternative electron flows (water-water cycle and cyclic electron  
515 flow around PS I) in photosynthesis: molecular mechanisms and physiological  
516 functions. *Plant and Cell Physiology* **51**, 1951-1963
- 517 Oguchi R, Douwstra P, Fujita T, Chow WS, Terashima I (2011) Intra-leaf gradients of  
518 photoinhibition induced by different color lights: Implications for the dual

- 519 mechanisms of photoinhibition and for the application of conventional chlorophyll  
520 fluorometers. *New Phytologist* **191**, 146–159
- 521 Öquist G, Chow, WS (1992) On the relationship between the quantum yield of  
522 Photosystem II electron transport, as determined by chlorophyll fluorescence and  
523 the quantum yield of CO<sub>2</sub>-dependent O<sub>2</sub> evolution. *Photosynthesis Research* **33**,  
524 51-62
- 525 Oxborough K, Baker NR (1997) Resolving chlorophyll *a* fluorescence images of  
526 photosynthetic efficiency into photochemical and non-photochemical  
527 components-calculation of  $qP$  and  $F_v'/F_m'$  without measuring  $F_o'$ . *Photosynthesis*  
528 *Research* **54**, 135–142
- 529 Seaton GGR, Walker DA (1990) Chlorophyll fluorescence as a measure of  
530 photosynthetic carbon assimilation. *Proceedings of the Royal Society of London B:*  
531 *Biological Sciences* **242**, 29-35
- 532 Shikanai T (2007) Cyclic electron transport around photosystem I: genetic approaches.  
533 *Annual Review of Plant Biology* **58**, 199-217
- 534 Terashima I, Fujita T, Inoue T, Chow WS, Oguchi R (2009) Green light drives leaf  
535 photosynthesis more efficiently than red light in strong white light: Revisiting the  
536 enigmatic question of why leaves are green. *Plant and Cell Physiology* **50**,  
537 684-697
- 538 Weis E, Berry JA (1987) Quantum efficiency of Photosystem II in relation to

539 'energy'-dependent quenching of chlorophyll fluorescence. *Biochimica et*  
540 *Biophysica Acta* **894**, 198-208

541 Yao H-S, Zhang, Y-L, Yi X-P, Zhang X-J, Fan D-Y, Chow WS, Zhang, W-F (2018)  
542 Diaheliotropic leaf movement enhances leaf photosynthetic capacity and  
543 photosynthetic use efficiency of light and photosynthetic nitrogen via optimizing  
544 nitrogen partitioning among photosynthetic components in cotton (*Gossypium*  
545 *hirsutum* L.). *Plant Biology*. DOI: 10.1111/plb.12678

546 Yi X-P, Zhang Y-L, Yao H-S, Han J-M, Chow WS, Fan D-Y, Zhang W-F (2018)  
547 Changes in activities of both photosystems and the regulatory effect of cyclic  
548 electron flow in field-grown cotton (*Gossypium hirsutum* L) under water deficit.  
549 *Journal of Plant Physiology* **220**, 74-82

550

551

552

553 **Table 1. Estimate of the fraction of absorbed light partitioned to PS II ( $f_{II}$ ) in leaf**  
 554 **discs in 1% CO<sub>2</sub>.** The average irradiance of modulated excitation was 0.05  $\mu\text{mol m}^{-2}$   
 555  $\text{s}^{-1}$  for blue or red excitation, and varied for green excitation (average irradiance in  
 556 parentheses)

Spinach			Excitation light				
Actinic irradiance	blue	red	Green (0.05)	Green (0.07)	Green (0.18)	Green (0.38)	Average
16	0.47	0.48	0.52	-	-	0.47	
38	0.46	0.47	0.52	-	-	0.51	
81	0.49	0.49	0.53	-	-	0.49	
163	0.53	0.50	0.54	-	-	0.50	
506	0.53	0.51	0.52	-	-	0.51	0.50±0.02 (sd)

557

Poplar			Excitation light				
Actinic irradiance	blue	red	Green (0.05)	Green (0.07)	Green (0.18)	Green (0.38)	Average
13	0.54	0.43	-	0.39	-	0.54	
33	0.47	0.43	-	0.37	-	0.53	
72	0.48	0.42	-	0.44	-	0.52	
145	0.50	0.52	-	0.47	-	0.52	0.47±0.05 (sd)

558

Rice			Excitation light				
Actinic irradiance	blue	red	Green (0.05)	Green (0.07)	Green (0.18)	Green (0.38)	Average
20	0.46	0.49	-	0.43	0.53	0.44	
41	0.54	0.51	-	0.49	0.47	0.53	
84	0.52	0.51	-	0.50	0.50	0.56	
169	0.51	0.49	-	0.50	0.48	0.52	
523	0.60	0.52	-	0.49	0.46	0.50	0.50±0.04 (sd)

559

Cotton			Excitation light				
Actinic irradiance	blue	red	Green (0.05)	Green (0.07)	Green (0.18)	Green (0.38)	Average
16	0.46	0.45	-	0.43	-	0.35	
36	0.49	0.46	-	0.47	-	0.43	
76	0.49	0.49	-	0.48	-	0.45	
152	0.51	0.51	-	0.50	-	0.49	0.47±0.04 (sd)

560

561

562

563

564

565 **Table 2**

566

567 **The difference between  $ETR_1$  and  $LEF_n$  ( $\Delta Flux$ ) in spinach leaf discs, as affected**  
 568 **by an inhibitor of cyclic electron transport or a mediator of oxygen reduction**

569

570 Leaf discs were vacuum infiltrated with water (control), 200  $\mu M$  AA or 100  $\mu M$  MV)  
 571 and, after evaporation of excess intercellular water, were illuminated at two  
 572 irradiances. Values are means for 3 to 4 leaf discs  $\pm$  s.d.

573

574

Treatment	$\Delta flux$	
	500 $\mu mol m^{-2} s^{-1}$	1000 $\mu mol m^{-2} s^{-1}$
water control	25.6 $\pm$ 4.6	77.9 $\pm$ 23.5
AA	2.3 $\pm$ 13.6	-3.4 $\pm$ 12.7
MV	0.3 $\pm$ 5.8	-10.4 $\pm$ 5.5

575

576

577

578

579

580 **Figure legends**

581 **Fig. 1.** Response of the linear photosynthetic electron flux of spinach leaf discs in 1%  
582 CO<sub>2</sub> to the irradiance of actinic light from a halogen lamp. The linear electron flux  
583 was measured either as the gross rate of oxygen evolution multiplied by 4 (●) or Chl  
584 fluorescence excited by modulated light from light-emitting diodes emitting at blue  
585 (◆, 0.05 μmol m<sup>-2</sup> s<sup>-1</sup>), red (■, 0.05 μmol m<sup>-2</sup> s<sup>-1</sup>) or green wavelengths (△, 0.05  
586 μmol m<sup>-2</sup> s<sup>-1</sup>; ▲, 0.38 μmol m<sup>-2</sup> s<sup>-1</sup>). Values are means of six to seven leaf discs (±  
587 s.d.).

588 **Fig. 2.** Response of the linear photosynthetic electron flux of poplar leaf discs in 1%  
589 CO<sub>2</sub> to the irradiance of actinic light from a halogen lamp. The linear electron flux  
590 was measured either as the gross rate of oxygen evolution multiplied by 4 (●, first  
591 batch of plants; ○, second batch of plants) or Chl fluorescence excited by modulated  
592 light from light-emitting diodes emitting at blue (◆, 0.05 μmol m<sup>-2</sup> s<sup>-1</sup>), red (■, 0.05  
593 μmol m<sup>-2</sup> s<sup>-1</sup>) or green wavelengths (△, 0.07 μmol m<sup>-2</sup> s<sup>-1</sup>, first batch of plants; ▲,  
594 0.38 μmol m<sup>-2</sup> s<sup>-1</sup>, second batch of plants). Values are means of nine to ten leaf  
595 discs (± s.d.).

596 **Fig. 3.** Response of the linear photosynthetic electron flux of rice leaf segments in 1%  
597 CO<sub>2</sub> to the irradiance of actinic light from a halogen lamp. The linear electron flux  
598 was measured either as the gross rate of oxygen evolution multiplied by 4 (●) or Chl  
599 fluorescence excited by modulated light from light-emitting diodes emitting at green

600 wavelengths ( $\Delta$ ,  $0.07 \mu\text{mol m}^{-2} \text{s}^{-1}$ ;  $\diamond$ ,  $0.18 \mu\text{mol m}^{-2} \text{s}^{-1}$ ;  $\blacktriangle$ ,  $0.38 \mu\text{mol m}^{-2} \text{s}^{-1}$ ).

601 Values are means of five to six leaf discs ( $\pm$  s.d.).

602 **Fig. 4.** Response of the linear photosynthetic electron flux of cotton leaf discs in 1%

603  $\text{CO}_2$  to the irradiance of actinic light from a halogen lamp. The linear electron flux

604 was measured either as the gross rate of oxygen evolution multiplied by 4 ( $\bullet$ ) or Chl

605 fluorescence excited by modulated light from light-emitting diodes emitting at blue

606 ( $\blacklozenge$ ,  $0.05 \mu\text{mol m}^{-2} \text{s}^{-1}$ ), red ( $\blacksquare$ ,  $0.05 \mu\text{mol m}^{-2} \text{s}^{-1}$ ) or green wavelengths ( $\Delta$ ,  $0.07$

607  $\mu\text{mol m}^{-2} \text{s}^{-1}$ ;  $\blacktriangle$ ,  $0.38 \mu\text{mol m}^{-2} \text{s}^{-1}$ ). Values are means of six leaf discs ( $\pm$  s.d.).

608 **Fig. 5.** Response of the total photosynthetic electron flux through PSI, ETR1 ( $\blacksquare$ )

609 and the Chl fluorescence-based linear photosynthetic electron flux through both

610 photosystems,  $\text{LEF}_{\text{fl}}$  ( $\bullet$ ) of spinach leaves attached to the plant in air (a) or leaf discs

611 in 1%  $\text{CO}_2$  (b). The difference between ETR1 and  $\text{LEF}_{\text{fl}}$  is  $\Delta\text{Flux}$  ( $\blacktriangle$ ), used as an

612 estimate of the cyclic electron flux around PSI. Values are means of seven leaves ( $\pm$

613 s.d.).

614 **Fig. 6.** Response of the total photosynthetic electron flux through PSI, ETR1 ( $\blacksquare$ )

615 and the Chl fluorescence-based linear photosynthetic electron flux through both

616 photosystems,  $\text{LEF}_{\text{fl}}$  ( $\bullet$ ) of poplar leaves attached to a branch of the plant in air (a) or

617 of leaf discs in 1%  $\text{CO}_2$  (b). The difference between ETR1 and  $\text{LEF}_{\text{fl}}$  is  $\Delta\text{Flux}$  ( $\blacktriangle$ ),

618 used as an estimate of the cyclic electron flux around PSI. Values are means of

619 seven leaves ( $\pm$  s.d.).

620 **Fig. 7.** Response of the total photosynthetic electron flux through PSI, ETR1 ( $\blacksquare$ )



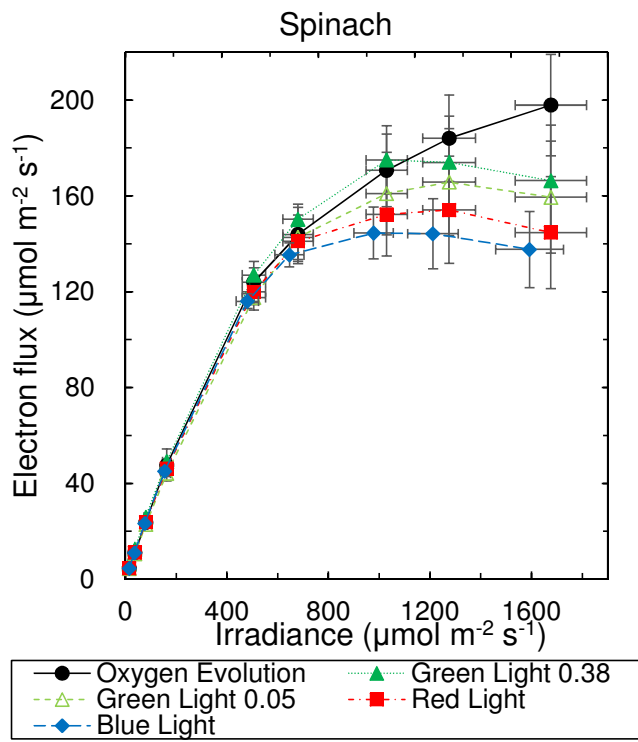
621 and the Chl fluorescence-based linear photosynthetic electron flux through both  
622 photosystems,  $LEF_{fl}$  (●) of rice leaves attached to the plant in air (a) or of leaf  
623 segments in 1%  $CO_2$  (b). The difference between ETR1 and  $LEF_{fl}$  is  $\Delta Flux$  (▲),  
624 used as an estimate of the cyclic electron flux around PSI. Values are means of  
625 seven leaves ( $\pm$  s.d.).

626 **Fig. 8.** Response of the total photosynthetic electron flux through PSI, ETR1 (■)  
627 and the Chl fluorescence-based linear photosynthetic electron flux through both  
628 photosystems,  $LEF_{fl}$  (●) of cotton leaves attached to the plant in air (a) or of leaf discs  
629 in 1%  $CO_2$  (b). The difference between ETR1 and  $LEF_{fl}$  is  $\Delta Flux$  (▲), used as an  
630 estimate of the cyclic electron flux around PSI. Values are means of seven leaves ( $\pm$   
631 s.d.).

632 **Fig. 9.** A plot of  $qP \times I$  (a) and  $F_v'/F_m' \times I$  (b) against irradiance  $I$  for cotton leaf  
633 discs in 1%  $CO_2$ . Values are means of nine leaves ( $\pm$  s.d.).

634

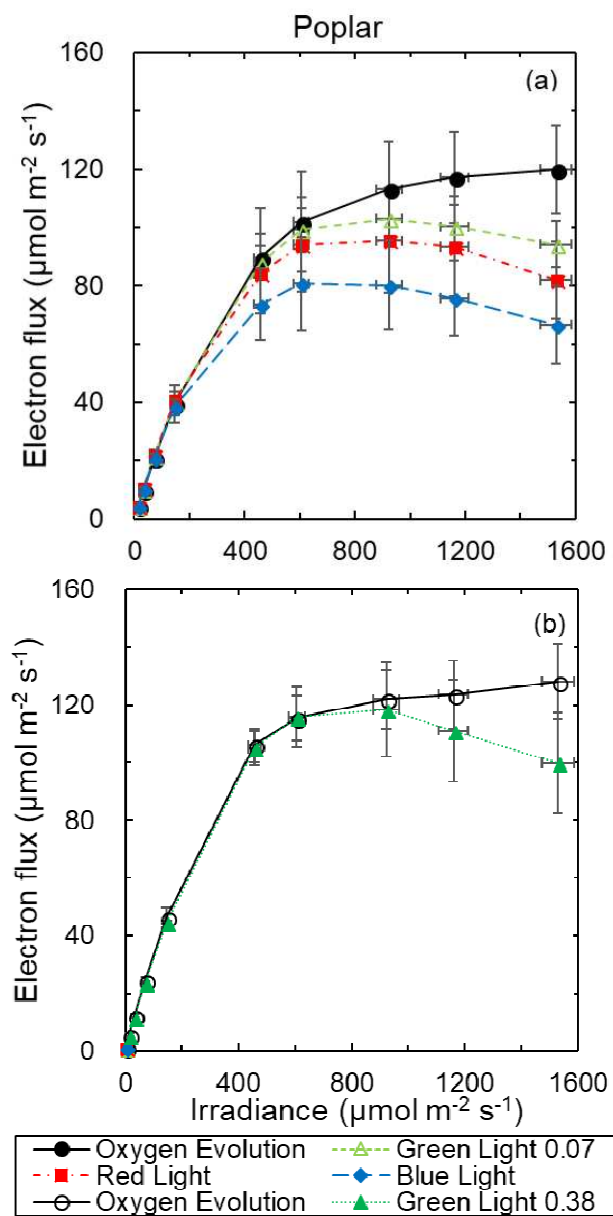
635 **Fig. 1**  
636  
637



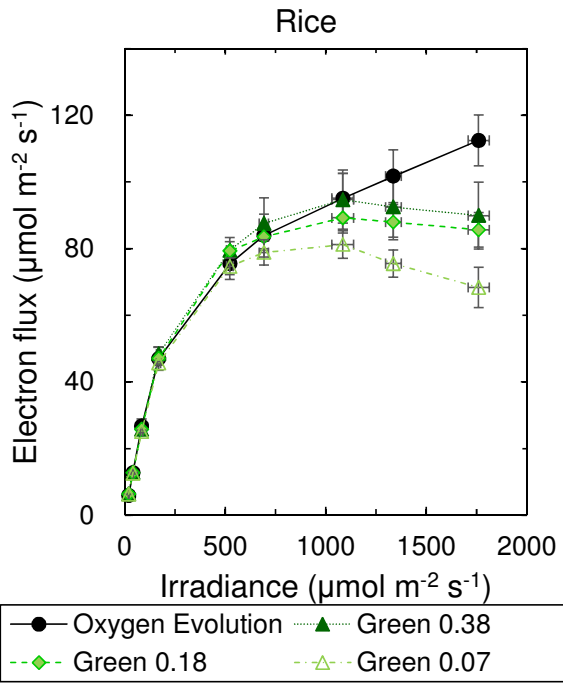
638  
639  
640

641 **Fig. 2**

642  
643  
644  
645  
646  
647  
648  
649  
650  
651  
652  
653  
654  
655  
656  
657  
658  
659  
660  
661

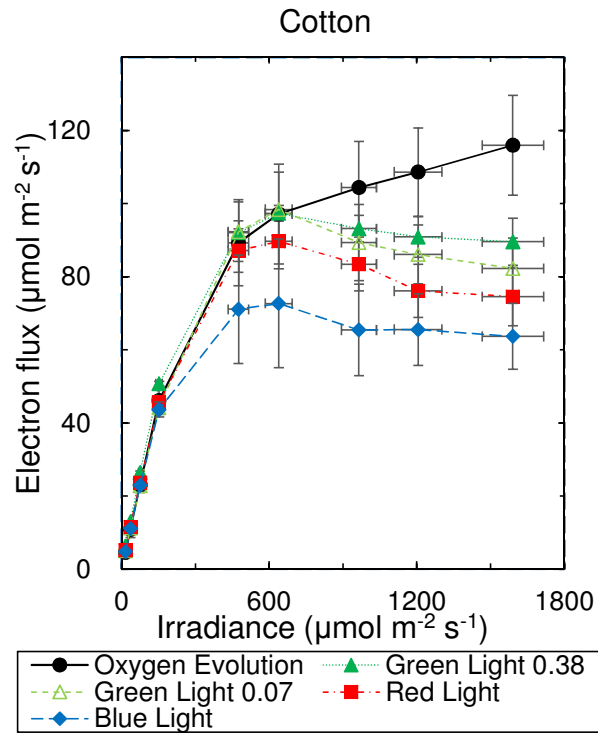


662 **Fig. 3**  
663



664  
665  
666  
667

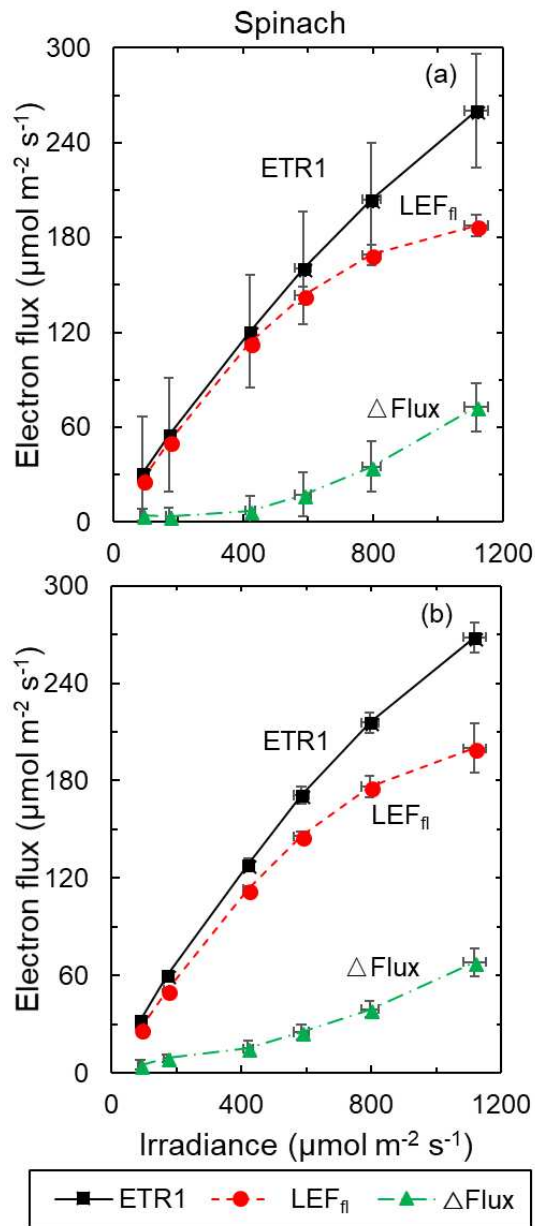
668 **Fig. 4**  
669  
670  
671  
672



673  
674  
675  
676

677 **Fig. 5**

678  
679  
680  
681  
682  
683  
684  
685  
686  
687  
688  
689  
690  
691  
692  
693  
694  
695  
696  
697  
698  
699  
700  
701  
702  
703  
704  
705  
706  
707  
708  
709  
710  
711  
712  
713  
714  
715  
716  
717  
718  
719



720  
721  
722  
723  
724  
725  
726  
727  
728  
729  
730  
731  
732  
733  
734  
735  
736  
737  
738  
739  
740  
741  
742  
743  
744  
745  
746  
747  
748  
749  
750  
751  
752  
753  
754  
755  
756  
757  
758  
759  
760  
761  
762

**Fig. 6**

**Comment [张1]:** Modify the graph

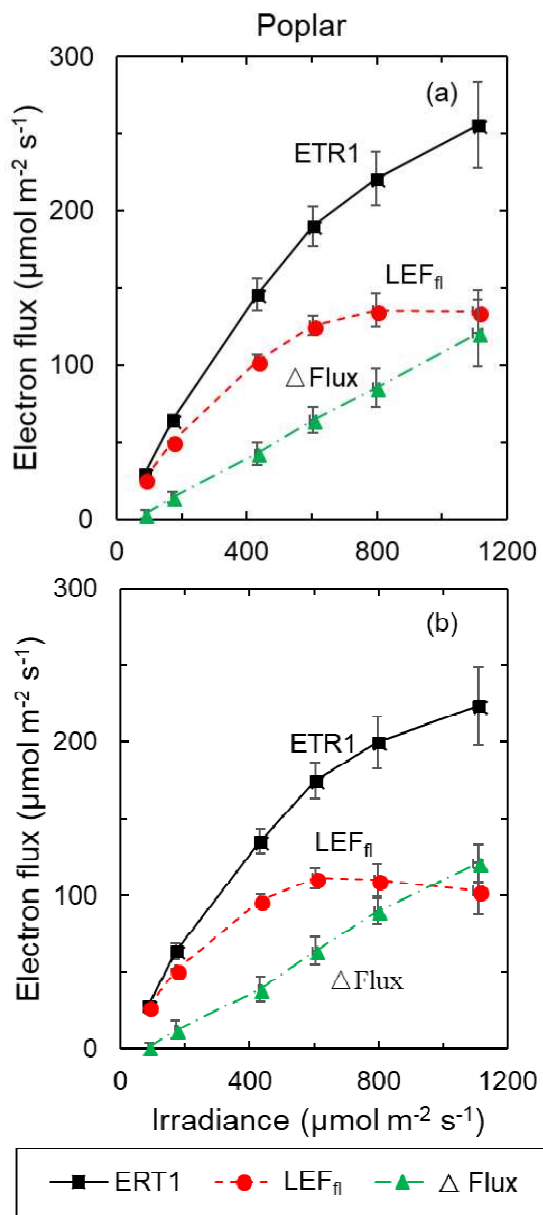
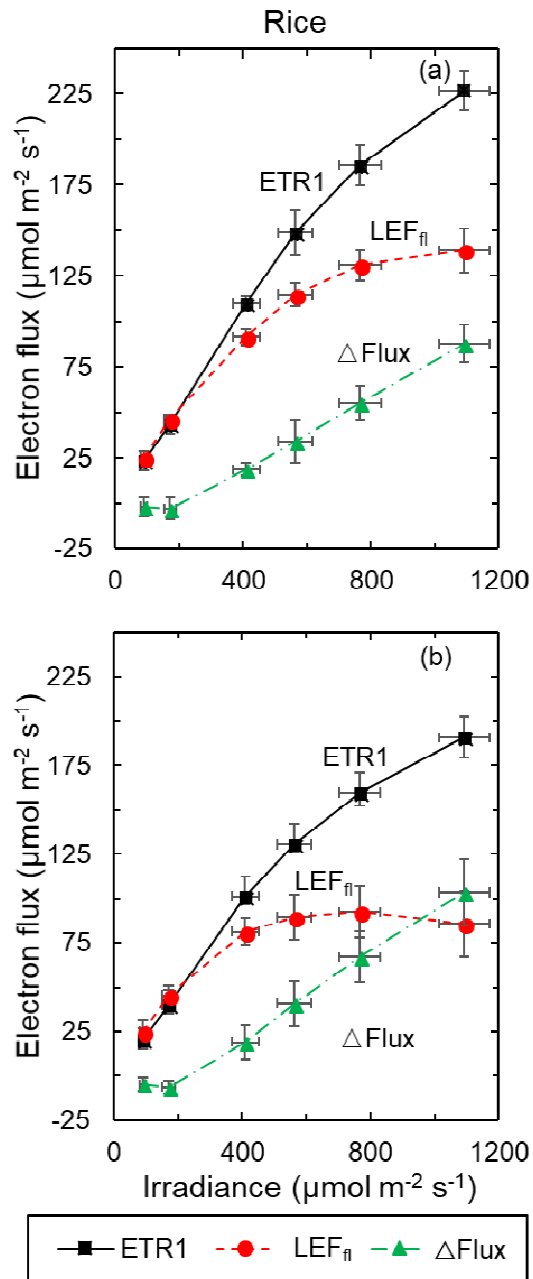


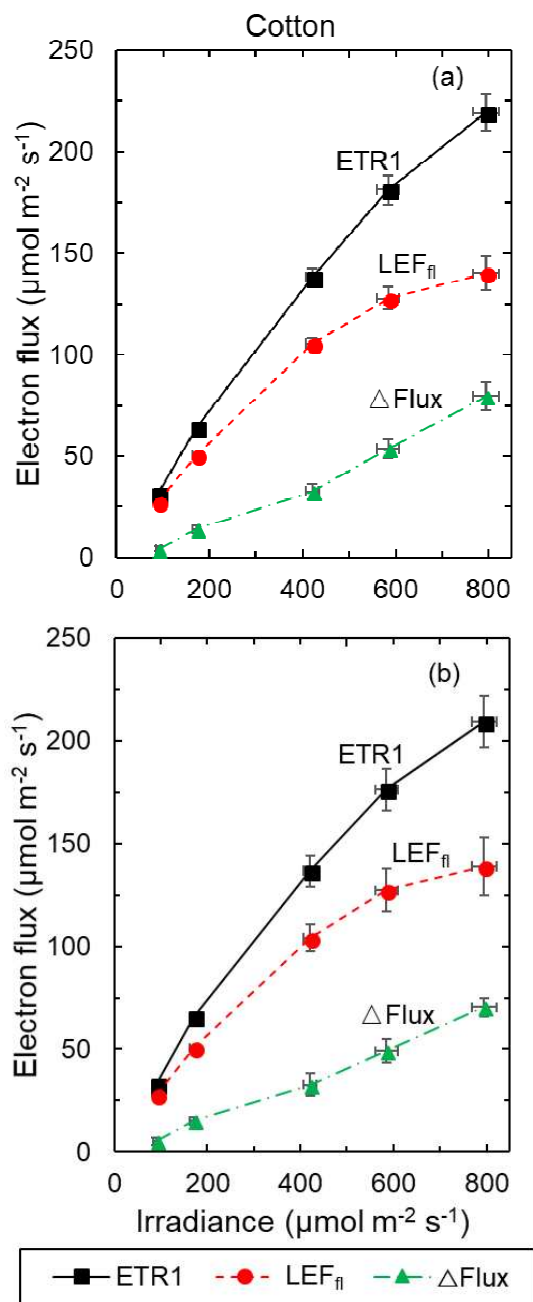
Fig. 7





807 **Fig. 8**

808  
809  
810  
811  
812  
813  
814  
815  
816  
817  
818  
819  
820  
821  
822  
823  
824  
825  
826  
827  
828  
829  
830  
831  
832  
833  
834  
835  
836  
837  
838  
839  
840  
841  
842  
843  
844  
845  
846  
847  
848  
849  
850



851 **Fig. 9**

852

853

854

855

856

857

858

859

860

861

862

863

864

865

866

867

868

869

870

871

872

873

874

875

876

877

878

879

880

881

